



## Migraine attacks as a result of hypothalamic loss of control

Anne Stankewitz<sup>a,b</sup>, Leonie Keidel<sup>b,d</sup>, Mathias Rehm<sup>b</sup>, Stephanie Irving<sup>a</sup>, Stephan Kaczmarz<sup>c</sup>,  
Christine Preibisch<sup>c</sup>, Viktor Witkovsky<sup>e</sup>, Claus Zimmer<sup>c</sup>, Enrico Schulz<sup>a,f,\*</sup>,  
Thomas R Toelle<sup>b,1</sup>

<sup>a</sup> Department of Neurology, Ludwig-Maximilians-Universität München, Munich, Germany

<sup>b</sup> Department of Neurology, Klinikum rechts der Isar, Technische Universität München, Munich, Germany

<sup>c</sup> Department of Neuroradiology, Klinikum rechts der Isar, Technische Universität München, Munich, Germany

<sup>d</sup> Department of Ophthalmology, Ludwig-Maximilians-Universität München, Munich, Germany

<sup>e</sup> Department of Theoretical Methods, Institute of Measurement Science, Slovak Academy of Sciences, Bratislava, Slovak Republic

<sup>f</sup> Department of Medical Psychology, Ludwig-Maximilians-Universität München, Munich, Germany

### ARTICLE INFO

#### Keywords:

Migraine  
Attacks  
Imaging  
Hypothalamus  
Limbic system

### ABSTRACT

Migraine is a complex neurological disorder affecting approximately 12% of the population. The pathophysiology is not yet fully understood, however the clinical features of the disease, such as the cyclic behaviour of attacks and vegetative symptoms, suggest a prominent role of the hypothalamus. Previous research has observed neuronal alterations at different time points during the migraine interval, specifically just before the headache is initiated. We therefore aimed to assess the trajectory of migraineurs' brain activity over an entire migraine cycle.

Using functional magnetic resonance imaging (fMRI) with pseudo-continuous arterial spin labelling (ASL), we designed a longitudinal intra-individual study to detect the rhythmicity of (1) the cerebral perfusion and (2) the hypothalamic connectivity over an entire migraine cycle. Twelve episodic migraine patients were examined in 82 sessions during spontaneous headache attacks with follow-up recordings towards the next attack.

We detected cyclic changes of brain perfusion in the limbic circuit (insula and nucleus accumbens), with the highest perfusion during the headache attack. In addition, we found an increase of hypothalamic connectivity to the limbic system over the interictal interval towards the attack, then collapsing during the headache phase.

The present data provide strong evidence for the predominant role of the hypothalamus in generating migraine attacks. Due to a genetically-determined cortical hyperexcitability, migraineurs are most likely characterised by an increased susceptibility of limbic neurons to the known migraine trigger. The hypothalamus as a metronome of internal processes is suggested to control these limbic circuits: migraine attacks may occur as a result of the hypothalamus losing control over the limbic system. Repetitive psychosocial stress, one of the leading trigger factors reported by patients, might make the limbic system even more vulnerable and lead to a premature triggering of a migraine attack. Potential therapeutic interventions are therefore suggested to strengthen limbic circuits with dedicated medication or psychological approaches.

### 1. Introduction

Migraine is a cyclic disease of attacks lasting 4 to 72 h and containing up to four phases: premonitory phase, migraine aura, headache phase, and the postdrome phase (Blau, 1992). Although the pathophysiology is not yet fully understood, strong evidence has emerged that both the peripheral trigemino-vascular system (Ashina et al., 2019) and the central nervous system contribute to the pathogenesis of migraine

(Harriott and Schwedt, 2014; Kros et al., 2018; May, 2017).

*Role of the hypothalamus in migraine.* The hypothalamus is involved in various cortical and subcortical circuits, such as limbic processes, circadian rhythms and hemostasis, and has been highlighted as a major player in initiating, maintaining, and remitting migraine attacks (Burstein et al., 2015; Karsan and Goadsby, 2018; May and Burstein, 2019; Nosedà and Burstein, 2013). The clinical features of migraine underline the hypothalamic contribution to the pathogenesis of the disease, i.e. the

\* Corresponding author: Ludwig-Maximilians-Universität München Neurologische Klinik und Poliklinik A Fraunhoferstr. 20, 82152 Martinsried, Germany.  
E-mail address: [es@pain.sc](mailto:es@pain.sc) (E. Schulz).

<sup>1</sup> These senior authors contributed equally to this study.

<https://doi.org/10.1016/j.nicl.2021.102784>

Received 23 April 2021; Received in revised form 6 July 2021; Accepted 6 August 2021

Available online 16 August 2021

2213-1582/© 2021 The Author(s).

Published by Elsevier Inc.

This is an open access article under the CC BY-NC-ND license

(<http://creativecommons.org/licenses/by-nc-nd/4.0/>).

cyclic behaviour of attacks, prodromal symptoms (yawning, fatigue, and mood changes), autonomous symptoms (nausea and vomiting), as well as trigger factors, such as certain hormones and psycho-physiological stress (Karsan and Goadsby, 2018; Pavlovic et al., 2014).

The first observations of an increased cerebral blood flow bilaterally in the hypothalamus during spontaneous headache attacks have been made with positron emission tomography (PET) (Denuelle et al., 2007). However, due to the unpredictable onset of migraine attacks, the investigation of the cyclic behaviour of hypothalamic activity is challenging and the group size of studies is therefore often limited (Schulte et al., 2020a; Stankewitz et al., 2011; Stankewitz and May, 2011).

*Studies on painful stimulation of the trigeminal system in migraine.* Functional magnetic resonance imaging (fMRI) studies have applied painful stimulation in order to stress the trigeminal system (Schulte et al., 2020a; Stankewitz et al., 2011). Investigating the effects of external stimuli instead of the more relevant endogenous pain is a known methodological limitation of functional imaging, as the change of cortical activity can only be determined in contrast to a baseline or to a functional control condition. Recently, a longitudinal fMRI study observed increased hypothalamic activity in response to painful stimulation during the 48 h prior to the beginning of headache attacks. By contrast, the hypothalamus was not active during the migraine attack (Schulte et al., 2020a). Using the same trigemino-nociceptive and olfactory stimulation design, previous studies did not find any hypothalamic alterations neither during (Stankewitz et al., 2011; Stankewitz and May 2011) nor within the last 72 h prior to spontaneous headache attacks (Stankewitz et al., 2011).

*Studies on hypothalamic functional connectivity in migraine.* Other fMRI studies have focussed on hypothalamic functional connections, finding stronger hypothalamic connectivity in response to painful trigeminal stimulation in migraineurs during headache attacks compared to the pain-free interval (Amin et al., 2018; Schulte and May 2016) and during the prodromal phase (24 h prior to spontaneous migraine headache; Meylakh et al., 2018; Schulte and May 2016). However, the very same methodological limitations apply; the natural cycle of the migraine is not being measured.

*Longitudinal fMRI studies on migraine without external stimulation.* Recently, the functional connectivities of nine migraineurs, recorded over the migraine cycle, were published based on resting-state data without any external stimulation. Ictally, increased connectivity was observed between the hypothalamus and the dorsal rostral pons compared to the interictal phase (Schulte et al., 2020b).

The present study was designed to circumvent the limitations of previous studies by combining two important aspects. First, we used a longitudinal design to assess the brain processes that change over an entire migraine cycle with a specific focus on the time series aspect of the data. Second, we followed the progress of the endogenous brain processes, untriggered and unstimulated. In addition, we focussed on two distinct brain processes: on the one hand we utilised the pseudo-continuous arterial spin labelling (pCASL) technique which allows the

non-invasive measurement of cerebral blood flow (CBF). On the other hand, seed-based resting state functional MRI was specifically used to trace rhythmic changes in hypothalamic connectivity throughout the entire brain.

## 2. Methods

### 2.1. Subjects

Twenty-two episodic migraine patients were included in the study (Table 1). Drop-outs from the initially-recruited subjects resulted from incidental MRI findings (n = 2), technical problems with the scanner hardware (n = 3) or software (n = 1), illness of patients (n = 2), or taking analgesic medication due to an acute painful event (n = 1) during the scanning period. One patient decided to withdraw prematurely from the study. In order to collect a sufficient amount of individual data for our longitudinal statistical analyses, we included patients with attack frequencies between 1 and 6 per month. One patient reported a frequency between 6 and 10 attacks per month, had a slightly shorter cycle, and was scanned almost daily. Fig. 1 shows the time course of the fMRI recordings for the 12 subjects (11f/1m; 3f with aura). The time points of the attacks were equally distributed in reference to the menstrual cycles of the female patients. Characteristics and clinical features are presented in Table 1. Migraine diagnosis was based upon the classification of the

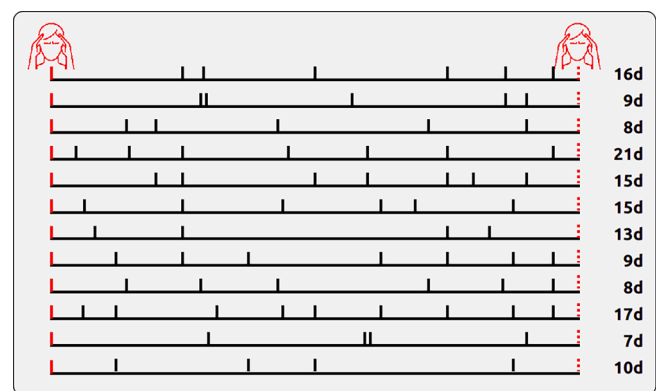


**Fig. 1.** Time course of individual recordings between two migraine attacks. Solid vertical lines indicate recording days. The dashed line at the end of the cycle represents the day of the subsequent migraine attack (not recorded) at which the recordings for the subjects were discontinued. The red lines indicate the attack days. The vertical black lines in between the attacks represent the recordings in the inter-ictal period. We recorded only one cycle per subject. The number of days between the first recorded migraine attack and the subsequent migraine attack is shown on the right and indicates the different length of each patient's migraine cycle. (For interpretation of the references to colour in this figure legend, the reader is referred to the web version of this article.)

**Table 1**  
Demographic characteristics and clinical migraine features.

| Patient | Age (years) | f/m | Attacks per month | Disease duration (years) | Attack severity (0–10) | Location of headache | With aura |
|---------|-------------|-----|-------------------|--------------------------|------------------------|----------------------|-----------|
| 1       | 28          | f   | 3–6               | 6                        | 6                      | right-sided          | yes       |
| 2       | 24          | m   | 3–6               | 14                       | 5–6                    | right-sided          | no        |
| 3       | 26          | f   | 3–6               | 24                       | 6                      | left-sided           | no        |
| 4       | 40          | f   | 1–2               | 29                       | 7–8                    | right-sided          | yes       |
| 5       | 32          | f   | 1–2               | 15                       | 6–7                    | right-sided          | no        |
| 6       | 30          | f   | 1–2               | 11                       | 7                      | bilateral            | no        |
| 7       | 22          | f   | 1–2               | 6                        | 5                      | left-sided           | no        |
| 8       | 23          | f   | 3–6               | 7                        | 8                      | bilateral            | no        |
| 9       | 33          | f   | 6–10              | 23                       | 8                      | right-sided          | no        |
| 10      | 26          | f   | 1–2               | 7                        | 5–7                    | left-sided           | no        |
| 11      | 21          | f   | 3–6               | 7                        | 8                      | bilateral            | yes       |
| 12      | 30          | f   | 1–2               | 14                       | 7                      | bilateral            | no        |

Attack severity was recorded on a numerical rating scale ranging from 0 (no pain) to 10 (highest imaginable pain).

International Headache Society (Headache Classification Committee of the International Headache Society (IHS), 2018). The patients did not report any other neurological or psychiatric disorders, were not taking preventative medication for migraine for at least six months, but were allowed to take their regular acute migraine medication after the recording of the headache attack (non-steroidal anti-inflammatory drugs or triptans). Due to their effects on cortical perfusion, patients were not permitted to consume coffee or other caffeinated beverages. All patients gave their written, informed consent. The study was conducted according to the Declaration of Helsinki and approved by the Ethics Committee of the Technische Universität München, Germany. All patients were remunerated for participation.

## 2.2. Study design

Migraine patients were tested repeatedly over an entire migraine cycle. The imaging time series for each patient started with the recording of a spontaneous and untreated headache attack within the first 6 h after the beginning of the headache. We only recorded headache attacks which were reported with an intensity of middle to strong, predefined as a minimum of “4” on a numerical rating scale with the endpoints “0” (no pain) and “10” (extremely intense pain). Brain perfusion images were then recorded every 1–4 days at the same time of the day until patients informed us by phone about the following headache attack (which was not scanned). The time series was completed with the last attack-free recording. We obtained data on the first day after the attack for all participants (12/12) and for the majority of the patients (9/12) on the day before or on the same day before the subsequent attack. All subjects had their final recording within 48 h before the subsequent attack.

## 2.3. Image acquisition

MRI data were collected on a 3 Tesla scanner (Ingenia, Philips, The Netherlands) using a 32-channel head coil. Patients were instructed to remain awake and relaxed with their eyes closed. The imaging parameters of the pseudocontinuous arterial spin labelling (pCASL) data were set according to the latest recommendations (Alsop et al., 2015). The labelling plane position was individually planned based on a phase contrast angiography (PCA) survey (scantime 0:21 min). The imaging parameters of the pCASL sequence were: labelling duration = 1650 ms; post label delay = 1700 ms; single-shot 2D EPI readout, repetition time (TR) = 5000 ms, time to echo (TE) = 16 ms; flip angle = 90°, 20 axial slices; field of view (FOV) = 240 mm × 240 mm × 119 mm<sup>3</sup>, voxel size = 2.73 × 2.73 × 5 mm<sup>3</sup>, gap 1 mm, 2 background suppression pulses, 50 repetitions. The total pCASL acquisition time corresponded to 8:30 min. Additionally, a proton density weighted (PDw) M<sub>0</sub> scan was acquired with TR = 5000 ms and 5 repetitions.

For the 300 volumes of resting state data, we used the following parameters: TR = 2000 ms; time to echo (TE) = 30 ms; FOV = 192 × 192 mm<sup>2</sup>; flip angle = 90°; number of slices = 37; voxel size = 3 × 3 × 3 mm<sup>3</sup> (0.29 mm gap). For image registration, a high resolution T1-weighted anatomical image was collected with: TR = 9000 ms, TE = 4 ms, flip angle = 8°, FOV = 240 × 240 × 170 mm<sup>3</sup>; number of slices = 170; voxel size = 1.0 × 1.0 × 1.0 mm<sup>3</sup>. Field maps were acquired in each session to control for B0-effects; 64 slices, TR = 960 ms, FOV = 192 × 192 mm<sup>2</sup>; voxel size = 2.0 × 2.0 × 2.0 mm<sup>3</sup>, 0.2 mm gap between slices. TE = 6 ms / 10.55 ms, flip angle 60°.

## 2.4. Data analysis

### 2.4.1. Cerebral blood perfusion (pCASL)

Quantitative cerebral blood flow (CBF) was derived from pCASL. Using SPM12 (Penny et al., 2011), all label and control images were motion corrected, averaged and subtracted to calculate perfusion weighted images. The M<sub>0</sub> image was derived from averaging the motion

corrected PDw images. By the perfusion weighted images and the M<sub>0</sub> image, quantitative CBF-maps were calculated according to recent recommendations (Alsop et al., 2015). Those CBF-maps were registered to MNI-space (2 mm isotropic resolution). As we were specifically interested in a very small subcortical region (the hypothalamus), we used a relatively small 3D Gaussian kernel with FWHM of 5 mm for spatial smoothing. Due to occasional artefacts in the vertex region, the analysis of CBF-maps was restricted to axial slices with z-coordinates < 58 mm.

### 2.4.2. Hypothalamic functional connectivity

The data were preprocessed with FSL. The Melodic toolbox was used to execute brain extraction, high-pass filtering with a frequency cutoff of 1/100 Hz, spatial registration to the MNI template, corrections for head motion during scanning, and a spatial smoothing (5 mm FWHM). A distortion correction of the images was used based on field maps. The data were further semi-automatically cleaned of artefacts with ICA through Melodic (Salimi-Khorshidi et al., 2014). The number of components had been automatically estimated by the software and artefact-related components were removed from the data according to the recommendations of Griffanti and colleagues (Griffanti et al., 2014). Head movement during scanning did not exceed 2 mm or 2° in any direction.

The hypothalamic spherical region of interest (ROI:  $x = 6/y = 0/z = -12, r = 5$  mm) was generated according to the MRI atlas of the human hypothalamus (Baroncini et al., 2012). The ROI was created in MNI standard space and transformed into the native space for each recording session and the mean time course of the hypothalamic activity was extracted. By using the FEAT toolbox, the blood oxygenation level dependent (BOLD) functional connectivity was computed in native space for each voxel by relating the time course of hypothalamus BOLD signal intensity to the time course of all voxels. Connectivity maps were subsequently transformed into MNI standard space for statistical analysis in Matlab.

### 2.4.3. Statistical analyses

The statistical analyses are identical for perfusion data and connectivity data. We explored the cyclic change of cortical perfusion and cortical connectivity over the migraine interval. In order to investigate how both aspects of cortical processing (perfusion, hypothalamic connectivity) evolve over the migraine cycle, we computed voxel-wise linear mixed effects models (LME) and related the time points within the migraine cycle to the rank-normalised brain processes (perfusion, hypothalamic connectivity) of interest separately for each voxel. We created a time vector for each patient's migraine cycle and encoded the day of the recording by assigning numbers between 1 and 2. The numbers 1 or 2 were assigned to the measurement during the headache attack, depending on the following two different time courses of migraine-related processes in the brain. For the two time courses, we utilised the term “trajectory” in order to emphasise the active and inevitable progress of the migraine cycle that ultimately leads to a migraine attack (Fig. 2).

Trajectory 1 (“reset mode”): In this model, we aimed to detect the migraine-related activity or connectivity that has its peak (positive or negative) just before the headache attack starts and then drops to the baseline level (positive or negative) during the headache. From here, the activity or connectivity linearly increases (or decreases) over the migraine cycle to the next attack. In this hypothetical time series, the brain activity or connectivity on the first day after the attack would be similar to the brain activity during the attack. This trajectory can be interpreted as a cortical “reset” mechanism and is in line with neurophysiological studies reporting a habituation deficit in pain-free migraineurs that normalise during headache attacks (Coppola et al., 2013, 2010; Schoenen et al., 1995). For 5 measurements over 10 days, the following vector is used to reflect the trajectory 1: 1 (=attack), 1.2, 1.4, 1.6, 1.8.

Trajectory 2 (“pain mode”): In this model, those migraine-related brain processes are aimed to be detected that have a peak during the

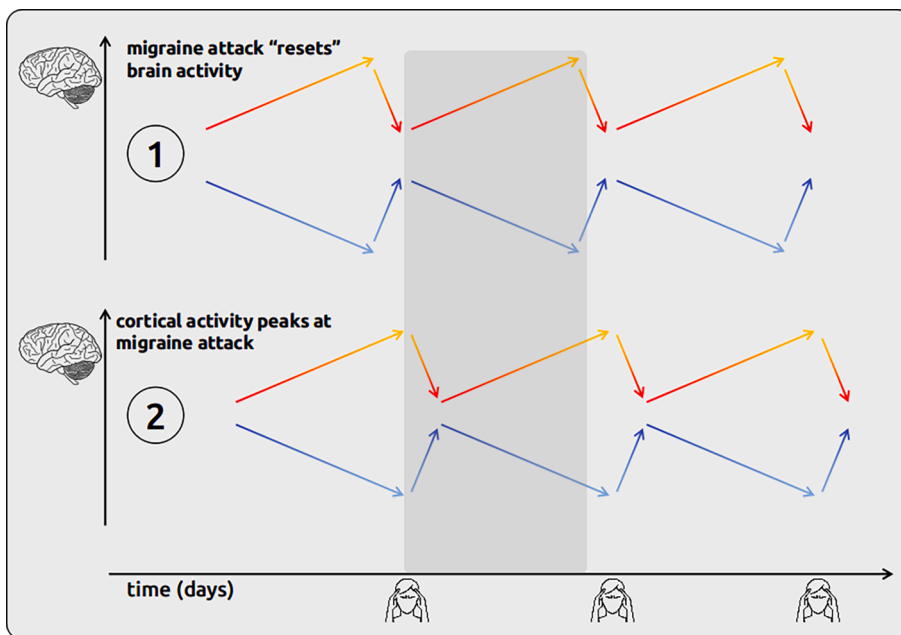


**Fig. 2.** Time series of migraine-related brain processes. Two hypothetical time series (trajectories) of migraine-related brain processes were modelled in the statistical analysis. In the first time series (upper part) the brain processes drop during the headache attacks; the brain processes would be “reset” during attacks, then would resemble the processes on the day after the attacks. In the second time series (lower part), the brain processes would reach their minimum/maximum during the attacks and are similar to the days before attacks. These processes could be used as a biomarker for an impending migraine attack. The figure is intended to illustrate the cyclic nature of migraine attacks and time-varying magnitude of two potential brain processes; we recorded only one migraine cycle (grey area).

headache attack and drop to the level (positive or negative) on the next day. From there, we assume a linear increase (or decrease) over the migraine cycle towards the next attack. We hypothesise increased brain activity in regions that contribute to the processing of migraine symptoms, e.g. pain, increased sensitivity to light, sound, and odors and vegetative complaints. In this hypothetical time series, the brain activity on the day prior to the attack would be similar to the brain activity during the headache attack and is suggested to reflect the increasing excitability of the brain. Similar to the above mentioned example with 5 measurements over 10 days, the following vector is used for the trajectory 2: 2 (=attack), 1.2, 1.4, 1.6, 1.8.

The statistical analysis for perfusion and for hypothalamic connectivity has been performed in Matlab (Version R2018a, Mathworks, USA). To explore the relationship between the fluctuating cortical connectivity and the variable pain experience, we computed LMEs (Schulz et al., 2019) that related the longitudinal recordings of perfusion and connectivity to the number vector of recording days:

$$(1) \text{ brain\_process} \sim \text{time} + (1|\text{subject})$$

The model is expressed in Wilkinson notation (Wilkinson and Rogers, 1973); the included fixed effect ( $\text{brain\_process} \sim \text{time}$ ) essentially describes the magnitudes of the population common intercept and the population common slope for the dependency of cortical data on the factor time. The added random effect (e.g.  $1 | \text{subject}$ ) is used to model the specific intercept differences for each subject. In other words, the model estimates the relationship between the brain processes in dependence on their occurrence in the migraine cycle (fixed effect). Please note that the statistical terms of fixed effect and random effect are differently used in the common neuroimaging software package SPM as compared with the standard nomenclature in statistics that we are following here. t-values are computed voxel-wise as quotients between the beta estimates and the standard errors of the equation. For a comprehensive introduction into LMEs, see (Harrison et al., 2018). The statistical threshold was set to  $p < 0.001$ . Patients were only included in the analysis if their movements did not exceed 2 mm in translation and  $2^\circ$  in rotation.

### 3. Results

#### 3.1. Cerebral blood perfusion (pCASL)

To determine the cyclic changes of the migraineurs’ brain activity between two migraine attacks, we computed a linear mixed effects (LME) model and analysed how the cortical perfusion (pCASL) is dependent upon the time point within the migraine cycle.

In the first part of our analyses we were testing for a “drop” of cortical activity during headache attacks (“reset mode”). We found that the superior parietal cortex showed significant cyclic activity, with lowest cortical perfusion during the headache that increased steadily afterwards (Table 2). There was no cyclic activity decreasing from the day of the attack for cortical perfusion.

Next, we tested for cortical activity that is changing towards the migraine attack and reaching its minimum/maximum during the attack (“pain mode”). We observed increasing blood perfusion with a maximum during the attack in the right insular cortex, the right nucleus accumbens, and the right precentral gyrus (Table 2 and Fig. 3). We did not find any cortical area that showed declining perfusion during the migraine attack.

#### 3.2. Hypothalamic functional connectivity

Based on previous research, we tested whether the hypothalamus is changing its functional connectivity over the migraine cycle. *First*, we tested for a “drop” of hypothalamic connectivity during headache attacks with a subsequent increase or decrease towards the next attack (“reset mode”). During the attack, we found a low hypothalamic connectivity to the limbic circuit (insula, parahippocampus, nucleus accumbens), the cerebellum, the basal ganglia loop, and sensory, and frontal cortices, which increased towards the next attack (Table 3 and Fig. 4). We did not find any significant effect for the opposite case, for which the hypothalamic connectivity would be high during the attack and steadily decreasing towards the next attack. *Next*, we tested for hypothalamic connectivity that is changing towards the attack and would reach its minimum/maximum during the attack (“pain mode”). Here, we did not find any significant results.

**Table 2**  
Brain perfusion data over the migraine cycle.

| Anatomical structures   | Cluster size |    | t values |      | MNI coordinates |     |    |    |    |     |  |
|-------------------------|--------------|----|----------|------|-----------------|-----|----|----|----|-----|--|
|                         | L            | R  | L        | R    | L               |     |    | R  |    |     |  |
|                         |              |    |          |      | x               | y   | z  | x  | y  | z   |  |
| Trajectory 1            |              |    |          |      |                 |     |    |    |    |     |  |
| Superior parietal gyrus | 33           |    | 3.7      |      | -12             | -34 | 54 |    |    |     |  |
| Trajectory 2            |              |    |          |      |                 |     |    |    |    |     |  |
| Precentral gyrus        |              | 13 |          | 3.56 |                 |     |    | 56 | 3  | 12  |  |
| Nucleus accumbens       |              | 11 |          | 3.4  |                 |     |    | 7  | 5  | -11 |  |
| Insula                  |              | 10 |          | 3.41 |                 |     |    | 43 | -8 | -6  |  |

Results of the LME model based on pCASL data (threshold  $p < 0.001$ ). Coordinates are in MNI space.

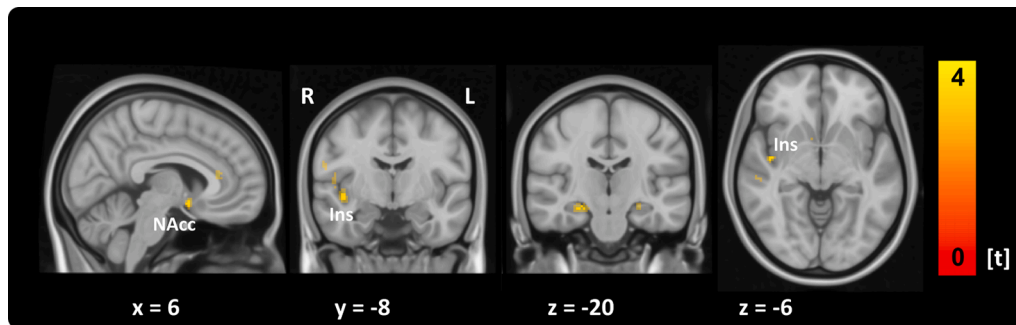


**Fig. 3.** Brain perfusion over the migraine cycle. Brain regions where perfusion is increased with closer temporal proximity to the next attack include limbic areas, particularly the insula and the nucleus accumbens. Bright colours represent a statistical threshold of  $p < 0.001$ , activities at a lowered threshold of  $p < 0.005$  have been included for display reasons in pale colours. NAcc = Nucleus accumbens, Ins = Insula, L = left; R = right.

**Table 3**  
Hypothalamic functional connectivity data over the migraine cycle.

| Anatomical structures          | Cluster size |    | t values |      | MNI coordinates |     |     |    |     |     |  |
|--------------------------------|--------------|----|----------|------|-----------------|-----|-----|----|-----|-----|--|
|                                | L            | R  | L        | R    | L               |     |     | R  |     |     |  |
|                                |              |    |          |      | x               | y   | z   | x  | y   | z   |  |
| Trajectory 1                   |              |    |          |      |                 |     |     |    |     |     |  |
| Cerebellum VIIb                | 90           | 59 | 3.85     | 3.99 | -24             | -67 | -53 | 22 | -68 | -55 |  |
| Occipital gyrus                |              | 14 |          | 3.79 |                 |     |     | 29 | -49 | -2  |  |
| Putamen                        | 42           |    | 3.88     |      | -22             | -3  | 11  |    |     |     |  |
| Pallidum                       | 40           |    | 4.01     |      | -21             | -5  | -3  |    |     |     |  |
| Postcentral gyrus              |              | 29 |          | 3.68 |                 |     |     | 65 | -16 | 28  |  |
| Cerebellum VI                  | 25           | 27 | 3.62     | 3.78 | -21             | -65 | -20 | 21 | -56 | -21 |  |
| Frontal pole                   | 20           | 27 | 3.8      | 3.67 | -38             | 45  | 33  | 45 | 37  | 14  |  |
| Cerebellum Crus I              |              | 25 |          | 3.61 |                 |     |     | 53 | -55 | -35 |  |
| Cerebellum VIIa                | 23           |    | 3.75     |      | -14             | -68 | -46 |    |     |     |  |
| Parietal cortex                |              | 22 |          | 3.54 |                 |     |     | 65 | -35 | 36  |  |
| Temporal Pole                  | 21           |    | 3.86     |      | -56             | 16  | -16 |    |     |     |  |
| Frontal inferior frontal gyrus |              | 20 |          | 3.47 |                 |     |     | 53 | 11  | 12  |  |
| Insula                         |              | 19 |          | 3.62 |                 |     |     | 45 | 11  | -2  |  |
| Insula                         |              | 16 |          | 3.62 |                 |     |     | 36 | -3  | 15  |  |
| Precentral gyrus               |              | 16 |          | 3.77 |                 |     |     | 64 | 3   | 8   |  |
| Parahippocampal gyrus          |              | 14 |          | 3.67 |                 |     |     | 30 | 3   | -27 |  |
| Nucleus Caudatus               |              | 14 |          | 3.5  |                 |     |     | 7  | 12  | -1  |  |
| Frontal orbital gyrus          |              | 12 |          | 3.72 |                 |     |     | 40 | 33  | -1  |  |
| Nucleus Accumbens              |              | 11 |          | 3.52 |                 |     |     | 14 | 17  | -7  |  |
| Temporal gyrus                 |              | 10 |          | 3.58 |                 |     |     | 40 | -1  | -23 |  |

Results of the LME model based on resting state functional connectivity data (threshold  $p < 0.001$ ). Coordinates are in MNI space.

#### 4. Discussion

The present longitudinal study aimed to detect and record the endogenous and natural rhythmicity of brain activity over an entire migraine cycle by examining episodic migraine patients. Two aspects were specifically addressed: (1) In order to assess the cyclic behaviour of the brain activity in migraine patients, we utilised the innovative MRI-based pCASL technique. This allows for voxel-wise measurement of

blood perfusion as a proxy for neuronal activity, yet avoids the shortcomings of fMRI BOLD designs requiring a baseline for comparisons. We were able to follow the naturally evolving trajectory of migraine-related rhythmic brain activity without the need of external painful stimulation. We found increasing blood flow over the pain-free interval that reached its maximum during the spontaneous headache attack in the posterior insula and the nucleus accumbens. (2) We further mapped the fluctuating hypothalamic connectivity across the whole brain over the entire

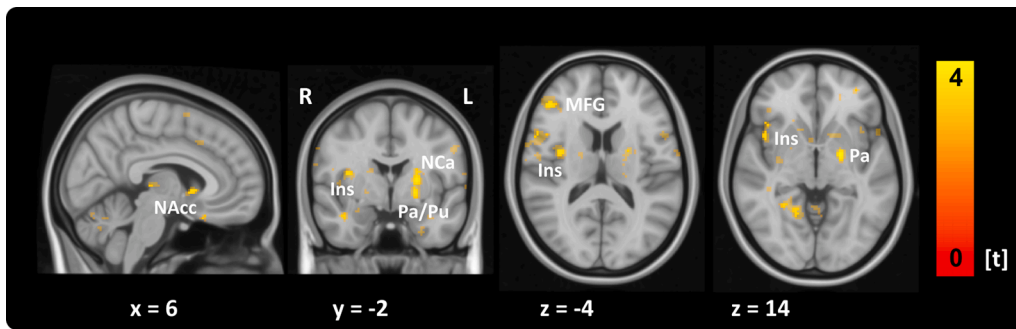


Fig. 4. Hypothalamic functional connectivity over the migraine cycle. Brain areas that are functionally connected with the hypothalamus with rhythmic changes over the migraine cycle: These connections are collapsing during the attack and are increasing towards the next attack. This connectivity profile relates to limbic areas, including the insula and the nucleus accumbens, as well as to basal ganglia and frontal areas. Bright colours represent a statistical threshold of  $p < 0.001$ , activities at a lowered threshold of  $p < 0.005$  have been included for display reasons in pale colours. NAcc = Nucleus accumbens,

Ins = Insula, MFG = Middle Frontal Gyrus, Pa = Pallidum, Pu = Putamen, L = left, R = right.

migraine cycle. Here, we observed the connectivity between the hypothalamus and the insula as well as the nucleus accumbens increased over the interictal interval, reaching its maximum shortly before the headache is initiated. In contrast, during the headache this connectivity was low, suggesting a hypothalamo-limbic connectivity collapse. Similar results were found for hypothalamic connections to the basal ganglia (nucleus caudatus, pallidum, and putamen), and cerebellar regions.

#### 4.1. Trajectory of the cerebral blood flow over the migraine cycle

Our longitudinal data over the migraine cycle shows that the perfusion changes occur mainly in limbic structures. We found increasing limbic activity towards the next attack that reached its peak during the migraine attack. This finding most likely reflects a steadily increasing sensitivity of the migraineurs' brain for sensory stimulation (Peng and May 2019). The limbic system is a collection of distinct but highly interconnected brain regions that contribute to the processing of fear (Sah, 2017), stress reactivity (Franklin et al., 2012), learning, and memory (Catani et al., 2013). Via its strong connections to subcortical and prefrontal areas, the limbic system is considered to be a mediator between autonomic reactions and the cognitive evaluation of incoming aversive sensory stimuli (Wager et al., 2008; Wilcox et al., 2016).

In migraine, clinical observations (Blau, 1980) and experimental research (Karsan and Goadsby, 2018) point to a deviant processing of sensory stimuli, which can be attributed to the impaired limbic system. Particularly during attacks, patients report an enhanced sensitivity to sensory input irrespective of the modality (light, sound, odour, and sensation), causing many patients to prefer a dark and quiet environment (Headache Classification Committee of the International Headache Society (IHS), 2018). Altered sensory perception, including pain, is not limited to the ictal phase, but has also been observed during the pain-free interval (Peng and May 2019). Several electrophysiological studies demonstrated a lack of habituation in migraineurs interictally in response to repetitive sensory stimulation (Ozkul and Uckardes, 2002; Schoenen et al., 1995; Siniatchkin et al., 2006; Valeriani et al., 2003; Wang et al., 1996). In contrast, the habituation deficit normalised just before and during attacks (Chen et al., 2009; Judit et al., 2000). Due to its important role in integrating incoming stimuli, an impaired limbic system is most likely responsible for the altered sensory processing in migraine patients (Liu et al., 2018; Maizels et al., 2012). Functional MRI studies revealed enhanced limbic activity during migraine attacks in response to painful (Moulton et al., 2011) and olfactory stimulation (Stankewitz and May 2011). In contrast, hypometabolism of limbic areas, particularly the insula, cingulate and prefrontal cortices, was observed during the pain-free interval, compared to healthy controls (Kim et al., 2010). Other studies observed an altered functional connectivity between the hippocampus, insula, amygdala, and pain-modulating and encoding areas during (Amin et al., 2018; Coppola et al., 2018) and outside of migraine attacks (Wei et al., 2019).

Further clinical evidence for a migraine-related cyclic trajectory of the limbic system comes from studies on psycho-physiological stress. Processed in limbic structures, psycho-physiological stress is one of the predominant factors for the initiation of the attack (Pavlovic et al., 2014). Stress-related symptoms accompanying the headache, such as reactions of the autonomic nervous system as well as cognitive and attentional deficits, have been linked to limbic processes (Herman et al., 2005; Jankord and Herman, 2008; Morgane et al., 2005). Limbic alterations are further related to migraine-related disabilities (Wei et al., 2019), increased pain during attacks (Coppola et al., 2018) and the severity of the disease (Kim et al., 2010; Mainero et al., 2011). These findings offer the opportunity to tailor migraine treatments specifically to limbic functions. Cognitive strategies (Ng et al., 2017; Seng and Holroyd, 2014), relaxation methods (Meyer et al., 2016), and biofeedback (Stubberud et al., 2016) were shown to be effective techniques to reduce the acute pain sensation and the headache frequency in migraineurs.

Taken together, our findings suggest a cyclic dysfunction of the limbic system. In migraineurs, the limbic system may be genetically determined to be highly vulnerable for sensory input due to ion channel alterations (Kullmann and Hanna, 2002). The increasing cerebral blood flow in the limbic system over the migraine cycle may reflect an increasing cortical responsiveness to external stimuli. As a result, an impaired limbic function might lead to a general sensory overload in the cortex during the attack, causing a variety of clinical symptoms. The hypothalamus, considered to be a metronome of the limbic circuit, is suggested to be a candidate for triggering the observed rhythmic changes of the limbic activity.

#### 4.2. Hypothalamic functional connectivity over the migraine cycle

There is strong evidence that the hypothalamus is substantially involved in the pathogenesis of migraine attacks (Karsan and Goadsby, 2018; May and Burstein, 2019). Clinical features of the disease correspond to the rhythmic functions of the hypothalamus (Karsan and Goadsby, 2018; Pavlovic et al., 2014). Therefore, we specifically addressed the fluctuations of hypothalamic connections within the brain over the entire migraine cycle. We observed the functional connectivity between the hypothalamus and other limbic centres increased linearly over the interictal interval, reaching its peak shortly before a headache is initiated. In contrast, we found this connectivity to be disturbed during the attack. Similar results were observed for hypothalamic connections to the basal ganglia and cerebellar regions.

The hypothalamus is highly connected with multiple brain regions, including the limbic pathway (Noseda and Burstein, 2013). It controls the autonomous and the endocrine system and regulates the haemostatic balance (Hastings et al., 2007; Holland et al., 2018). These functions are closely related to symptoms during attacks (nausea, vomiting, fatigue, polyuria) and to trigger factors reported by migraine patients, such as

changes in hormone status (including menstruation), an unbalanced sleep-wake rhythm, or skipping a meal (Pavlovic et al., 2014). Alterations of the hypothalamus have been observed in previous neuroimaging research: increased activity was detected ictally (Denuelle et al., 2007; Schulte and May 2016) and during the prodromal phase shortly before the onset of pharmacologically-triggered (Maniyar et al., 2014) and spontaneous headache attacks occurred (Schulte et al., 2020a; Schulte and May 2016). In addition, enhanced hypothalamic-brainstem functional connectivity was observed during migraine attacks, which was already present shortly before the onset of pain. The current finding underpins the importance of the hypothalamo-limbic loop for the generation of migraine attacks. Increasing connectivity between the hypothalamus and limbic areas during the pain-free interval is suggested to reflect the increasing hypothalamic effort to orchestrate limbic subregions that process external and internal information. An insufficient inhibition of limbic excitability in migraineurs may therefore result in a gradual sensory overload of the brain, which is “reset” in a migraine attack. The gradually increasing (towards the attack) and finally disrupted (during the attack) hypothalamo-limbic connection suggests that the headache attack is the result of a loss of control by the hypothalamus to limbic structures. The increasing connectivity to the limbic system may compensate for the fading “grip” with even stronger connection attempts. This system is suggested to finally collapse, which is giving rise to a subsequent migraine attack and increased limbic perfusion.

The presented longitudinal MRI study highlights the role of the hypothalamus in generating migraine attacks. Our findings may suggest an increasing loss of hypothalamic control over limbic structures, which could result in an increased susceptibility of limbic neurons to the known migraine triggers. Repetitive psychosocial stress, one of the leading trigger factors reported by patients, might make the limbic system even more vulnerable and cause premature triggering of a migraine attack. The effects of some prophylactic migraine drugs, including antidepressants and antiepileptic drugs, on the attack frequency and severity might rely on the inhibition of these hypersensitive limbic circuits.

#### 4.3. Limitations

From the present data and analysis approach, we can not determine any causal influence of one brain region over the other. However, due to its prominent role as a biological clock of several cortical rhythms, we assume a control function of the hypothalamus over the limbic system. This assumption is based on previous findings but is nevertheless speculative and needs to be confirmed with methods that allow causal inferences.

The sample of 12 migraineurs in the present study is larger than previous attempts to investigate cyclic activity in migraine. Nevertheless, further studies with a larger sample and repeated cycles are needed to confirm the present exploratory findings. Such studies should allow for the investigation of the influence of the known factors that trigger headache attacks, such as stress level, hormones, sleep-awake rhythm, on hypothalamic and limbic connectivities.

In the present study, we did not distinguish between migraineurs with and without aura. Previous studies have shown some differences in cortical processing between these groups, however these studies do not assume a fundamental difference regarding the underlying cause of both types of migraine.

#### 5. Conclusions

The present longitudinal imaging study investigated the brain activity during the natural, unstimulated, migraine cycle in migraine patients. In line with previous findings, our data suggest that the hypothalamus is involved in the generation of headache attacks. We observed an increasing connectivity between the hypothalamus and

limbic areas over the interictal migraine interval towards the next attack that dropped during the headache. Given the predominant role of the hypothalamus as a biological clock, our data indicate that headache attacks are the result of the hypothalamus losing control over the limbic system. Potential therapeutic interventions are therefore suggested to strengthen limbic circuits with psychological approaches, such as relaxation techniques, cognitive interventions, or biofeedback.

#### Declaration of Competing Interest

The authors declare that they have no known competing financial interests or personal relationships that could have appeared to influence the work reported in this paper.

#### Acknowledgements

The study has been funded by the Else-Kröner-Fresenius Stiftung (Anne Stankewitz - 2014-A85).

Author contributions: A.S. and E.S. contributed to the conception and design of the study, acquisition and analysis of the data and drafting the manuscript and figures. L.K. contributed to the acquisition and analysis of the data. M.R. contributed to the acquisition and analysis of the data and drafting the manuscript and figures. S.I. contributed to drafting the manuscript.

S.K., C.P. and C.Z. contributed to the acquisition and analysis of the data. V.W. contributed to the analysis of the data. T.R.T. contributed to the conception and design of the study.

#### References

- Alsop, D.C., Detre, J.A., Golay, X., Günther, M., Hendrikse, J., Hernandez-Garcia, L., Lu, H., MacIntosh, B.J., Parkes, L.M., Smits, M., van Osch, M.J.P., Wang, D.J.J., Wong, E.C., Zaharchuk, G., 2015. Recommended implementation of arterial spin-labeled perfusion MRI for clinical applications: a consensus of the ISMRM perfusion study group and the European consortium for ASL in dementia. *Magn. Reson. Med.* 73, 102–116. <https://doi.org/10.1002/mrm.25197>.
- Amin, F.M., Hougaard, A., Magon, S., Sprenger, T., Wolfram, F., Rostrup, E., Ashina, M., 2018. Altered thalamic connectivity during spontaneous attacks of migraine without aura: a resting-state fMRI study. *Cephalalgia* 38, 1237–1244. <https://doi.org/10.1177/0333102417729113>.
- Ashina, M., Hansen, J.M., Do, T.P., Melo-Carrillo, A., Burstein, R., Moskowitz, M.A., 2019. Migraine and the trigeminovascular system—40 years and counting. *Lancet Neurol.* 18, 795–804. [https://doi.org/10.1016/S1474-4422\(19\)30185-1](https://doi.org/10.1016/S1474-4422(19)30185-1).
- Baroncini, M., Jissendi, P., Balland, E., Besson, P., Pruvo, J.-P., Francke, J.-P., Dewailly, D., Blond, S., Prevot, V., 2012. MRI atlas of the human hypothalamus. *Neuroimage* 59, 168–180. <https://doi.org/10.1016/j.neuroimage.2011.07.013>.
- Blau, J.N., 1980. Migraine prodromes separated from the aura: complete migraine. *Br. Med. J.* 281, 658–660. <https://doi.org/10.1136/bmj.281.6241.658>.
- Blau, J.N., 1992. Migraine: theories of pathogenesis. *Lancet* 339, 1202–1207. [https://doi.org/10.1016/0140-6736\(92\)91140-4](https://doi.org/10.1016/0140-6736(92)91140-4).
- Burstein, R., Nosedà, R., Borsook, D., 2015. Migraine: multiple processes, complex pathophysiology. *J. Neurosci.* 35, 6619–6629. <https://doi.org/10.1523/JNEUROSCI.0373-15.2015>.
- Catani, M., Dell'Acqua, F., Thiebaut de Schotten, M., 2013. A revised limbic system model for memory, emotion and behaviour. *Neurosci. Biobehav. Rev.* 37, 1724–1737. <https://doi.org/10.1016/j.neubiorev.2013.07.001>.
- Chen, W.-T., Wang, S.-J., Fuh, J.-L., Lin, C.-P., Ko, Y.-C., Lin, Y.-Y., 2009. Peri-ictal normalization of visual cortex excitability in migraine: an MEG study. *Cephalalgia* 29, 1202–1211. <https://doi.org/10.1111/j.1468-2982.2009.01857.x>.
- Coppola, G., Currà, A., Sava, S.L., Alibardi, A., Parisi, V., Pierelli, F., Schoenen, J., 2010. Changes in visual-evoked potential habituation induced by hyperventilation in migraine. *J. Headache Pain* 11, 497–503. <https://doi.org/10.1007/s10194-010-0239-7>.
- Coppola, G., Di Lorenzo, C., Schoenen, J., Pierelli, F., 2013. Habituation and sensitization in primary headaches. *J. Headache Pain* 14, 65. <https://doi.org/10.1186/1129-2377-14-65>.
- Coppola, G., Di Renzo, A., Tinelli, E., Di Lorenzo, C., Scapecchia, M., Parisi, V., Serrao, M., Evangelista, M., Ambrosini, A., Colonnese, C., Schoenen, J., Pierelli, F., 2018. Resting state connectivity between default mode network and insula encodes acute migraine headache. *Cephalalgia* 38, 846–854. <https://doi.org/10.1177/0333102417715230>.
- Denuelle, M., Fabre, N., Payoux, P., Chollet, F., Geraud, G., 2007. Hypothalamic activation in spontaneous migraine attacks. *Headache* 47:1418–1426. doi:10.1111/j.1526-4610.2007.00776.x.
- Franklin, T., Saab, B., Mansuy, I., 2012. Neural mechanisms of stress resilience and vulnerability. *Neuron* 75, 747–761. <https://doi.org/10.1016/j.neuron.2012.08.016>.

- Griffanti, L., Salimi-Khorshidi, G., Beckmann, C.F., Auerbach, E.J., Douaud, G., Sexton, C. E., Zsoldos, E., Ebmeier, K.P., Filippini, N., Mackay, C.E., Moeller, S., Xu, J., Yacoub, E., Baselli, G., Ugurbil, K., Miller, K.L., Smith, S.M., 2014. ICA-based artefact removal and accelerated fMRI acquisition for improved resting state network imaging. *Neuroimage* 95, 232–247. <https://doi.org/10.1016/j.neuroimage.2014.03.034>.
- Harriott, A.M., Schwedt, T.J., 2014. Migraine is associated with altered processing of sensory stimuli. *Curr. Pain Headache Rep.* 18, 458. <https://doi.org/10.1007/s11916-014-0458-8>.
- Harrison, X.A., Donaldson, L., Correa-Cano, M.E., Evans, J., Fisher, D.N., Goodwin, C.E. D., Robinson, B.S., Hodgson, D.J., Inger, R., 2018. A brief introduction to mixed effects modelling and multi-model inference in ecology. *PeerJ* 6:e4794. doi: 10.7717/peerj.4794.
- Hastings, M., O'Neill, J.S., Maywood, E.S., 2007. Circadian clocks: regulators of endocrine and metabolic rhythms. *J. Endocrinol.* 195, 187–198. <https://doi.org/10.1677/JOE-07-0378>.
- Herman, J.P., Ostrander, M.M., Mueller, N.K., Figueiredo, H., 2005. Limbic system mechanisms of stress regulation: hypothalamo-pituitary-adrenocortical axis. *Prog. Neuro-Psychopharmacol. Biol. Psychiatry* 29, 1201–1213. <https://doi.org/10.1016/j.pnpb.2005.08.006>.
- Holland, P., Barloese, M., Fahrenkrug, J., 2018. PACAP in hypothalamic regulation of sleep and circadian rhythm: importance for headache. *J. Headache Pain* 19, 1–8. <https://doi.org/10.1186/s10194-018-0844-4>.
- Headache Classification Committee of the International Headache Society (IHS). 2018. The International Classification of Headache Disorders, 3rd edition. *Cephalalgia* 38: 1–211. doi:10.1177/0333102417738202.
- Jankord, R., Herman, J.P., 2008. Limbic regulation of hypothalamo-pituitary-adrenocortical function during acute and chronic stress. *Ann. N. Y. Acad. Sci.* 1148, 64–73. <https://doi.org/10.1196/annals.1410.012>.
- Judit, Á., Sándor, P.S., Schoenen, J., 2000. Habituation of visual and intensity dependence of auditory evoked cortical potentials tends to normalize just before and during the migraine attack. *Cephalalgia* 20, 714–719. <https://doi.org/10.1111/j.1468-2982.2000.00122.x>.
- Karsan, N., Goadsby, P.J., 2018. Biological insights from the premonitory symptoms of migraine. *Nat. Rev. Neurol.* 14, 699–710. <https://doi.org/10.1038/s41582-018-0098-4>.
- Kim, J.H., Kim, S., Suh, S.-I., Koh, S.-B., Park, K.-W., Oh, K., 2010. Interictal metabolic changes in episodic migraine: a voxel-based FDG-PET study. *Cephalalgia* 30, 53–61. <https://doi.org/10.1111/j.1468-2982.2009.01890.x>.
- Kros, L., Angueyra Aristizabal, C.A., Khodakhah, K., 2018. Cerebellar involvement in migraine. *Cephalalgia* 38, 1782–1791. <https://doi.org/10.1177/0333102417752120>.
- Kullmann, D.M., Hanna, M.G., 2002. Neurological disorders caused by inherited ion-channel mutations. *Lancet Neurol.* 1, 157–166. [https://doi.org/10.1016/S1474-4422\(02\)00071-6](https://doi.org/10.1016/S1474-4422(02)00071-6).
- Liu, H.-Y., Chou, K.-H., Chen, W.-T., 2018. Migraine and the Hippocampus. *Curr. Pain Headache Rep.* 22, 13. <https://doi.org/10.1007/s11916-018-0668-6>.
- Mainero, C., Boshyan, J., Hadjikhani, N., 2011. Altered functional magnetic resonance imaging resting-state connectivity in periaqueductal gray networks in migraine. *Ann. Neurol.* 70, 838–845. <https://doi.org/10.1002/ana.22537>.
- Maizels, M., Aurora, S., Heinricher, M., 2012. Beyond neurovascular: migraine as a dysfunctional neurolimbic pain network. *Headache* 52, 1553–1565. <https://doi.org/10.1111/j.1526-4610.2012.02209.x>.
- Maniyar, F.H., Sprenger, T., Monteith, T., Schankin, C., Goadsby, P.J., 2014. Brain activations in the premonitory phase of nitroglycerin-triggered migraine attacks. *Brain* 137, 232–241. <https://doi.org/10.1093/brain/awt320>.
- May, A., 2017. Understanding migraine as a cycling brain syndrome: reviewing the evidence from functional imaging. *Neurol. Sci.* 38, 125–130. <https://doi.org/10.1007/s10072-017-2866-0>.
- May, A., Burstein, R., 2019. Hypothalamic regulation of headache and migraine. *Cephalalgia* 39, 1710–1719. <https://doi.org/10.1177/0333102419867280>.
- Meyer, B., Keller, A., Wöhlbier, H.-G., Overath, C.H., Müller, B., Kropp, P., 2016. Progressive muscle relaxation reduces migraine frequency and normalizes amplitudes of contingent negative variation (CNV). *J. Headache Pain* 17, 37. <https://doi.org/10.1186/s10194-016-0630-0>.
- Meylakh, N., Marciszewski, K.K., Di Pietro, F., Macefield, V.G., Macey, P.M., Henderson, L.A., 2018. Deep in the brain: Changes in subcortical function immediately preceding a migraine attack. *Hum. Brain Mapp.* 39, 2651–2663. <https://doi.org/10.1002/hbm.24030>.
- Morgane, P., Galler, J., Mokler, D., 2005. A review of systems and networks of the limbic forebrain/limbic midbrain. *Prog. Neurobiol.* 75, 143–160. <https://doi.org/10.1016/j.neurobio.2005.01.001>.
- Moulton, E.A., Becerra, L., Maleki, N., Pendse, G., Tully, S., Hargreaves, R., Burstein, R., Borsook, D., 2011. Painful heat reveals hyperexcitability of the temporal pole in interictal and ictal migraine States. *Cereb. Cortex* 21, 435–448. <https://doi.org/10.1093/cercor/bhq109>.
- Ng, Q.X., Venkatanarayanan, N., Kumar, L., 2017. A systematic review and meta-analysis of the efficacy of cognitive behavioral therapy for the management of pediatric migraine. *Headache* 57, 349–362. <https://doi.org/10.1111/head.13016>.
- Nosedá, R., Burstein, R., 2013. Migraine pathophysiology: anatomy of the trigeminovascular pathway and associated neurological symptoms, CSD, sensitization and modulation of pain. *Pain* 154 (Suppl), 1. <https://doi.org/10.1016/j.pain.2013.07.021>.
- Ozkul, Y., Uckardes, A., 2002. Median nerve somatosensory evoked potentials in migraine. *Eur. J. Neurol.* 9, 227–232. <https://doi.org/10.1046/j.1468-1331.2002.00387.x>.
- Pavlovic, J.M., Buse, D.C., Sollars, C.M., Haut, S., Lipton, R.B., 2014. Trigger factors and premonitory features of migraine attacks: summary of studies. *Headache* 54, 1670–1679. <https://doi.org/10.1111/head.12468>.
- Peng, K.-P., May, A., 2019. Migraine understood as a sensory threshold disease. *Pain* 160, 1494–1501. <https://doi.org/10.1097/j.pain.0000000000001531>.
- Penny, W.D., Friston, K.J., Ashburner, J.T., Kiebel, S.J., Nichols, T.E., 2011. *Statistical Parametric Mapping: The Analysis of Functional Brain Images*. Elsevier.
- Sah, P., 2017. Fear, anxiety, and the amygdala. *Neuron* 96, 1–2. <https://doi.org/10.1016/j.neuron.2017.09.013>.
- Salimi-Khorshidi, G., Douaud, G., Beckmann, C.F., Glasser, M.F., Griffanti, L., Smith, S. M., 2014. Automatic denoising of functional MRI data: combining independent component analysis and hierarchical fusion of classifiers. *Neuroimage* 90, 449–468. <https://doi.org/10.1016/j.neuroimage.2013.11.046>.
- Schoenen, J., Wang, W., Albert, A., Delwaide, P.J., 1995. Potentiation instead of habituation characterizes visual evoked potentials in migraine patients between attacks. *Eur. J. Neurol.* 2, 115–122. <https://doi.org/10.1111/j.1468-1331.1995.tb00103.x>.
- Schulte, L.H., May, A., 2016. The migraine generator revisited: continuous scanning of the migraine cycle over 30 days and three spontaneous attacks. *Brain* 139, 1987–1993. <https://doi.org/10.1093/brain/aww097>.
- Schulte, L.H., Mehnert, J., May, A., 2020a. Longitudinal neuroimaging over 30 days: temporal characteristics of migraine. *Ann. Neurol.* 87, 646–651. <https://doi.org/10.1002/ana.25697>.
- Schulte, L.H., Menz, M.M., Haaker, J., May, A., 2020b. The migraineur's brain networks: Continuous resting state fMRI over 30 days. *Cephalalgia* 40, 1614–1621. <https://doi.org/10.1177/0333102420951465>.
- Schulz, E., Stankewitz, A., Witkovský, V., Winkler, A.M., Tracey, I., 2019. Strategy-dependent modulation of cortical pain circuits for the attenuation of pain. *Cortex* 113, 255–266. <https://doi.org/10.1016/j.cortex.2018.12.014>.
- Seng, E.K., Holroyd, K.A., 2014. Behavioral migraine management modifies behavioral and cognitive coping in people with migraine. *Headache* 54, 1470–1483. <https://doi.org/10.1111/head.12426>.
- Siniatchkin, M., Averkina, N., Andrasik, F., Stephani, U., Gerber, W.-D., 2006. Neurophysiological reactivity before a migraine attack. *Neurosci. Lett.* 400, 121–124. <https://doi.org/10.1016/j.neulet.2006.02.019>.
- Stankewitz, A., May, A., 2011. Increased limbic and brainstem activity during migraine attacks following olfactory stimulation. *Neurology* 77, 476–482.
- Stankewitz, A., Aderjan, D., Eippert, F., May, A., 2011. Trigeminal Nociceptive transmission in migraineurs predicts migraine attacks. *J. Neurosci.* <https://doi.org/10.1523/JNEUROSCI.4496-10.2011>.
- Stubberud, A., Varkey, E., McCrory, D.C., Pedersen, S.A., Linde, M., 2016. Biofeedback as Prophylaxis for Pediatric Migraine: A Meta-analysis. *Pediatrics* 138, e20160675. <https://doi.org/10.1542/peds.2016-0675>.
- Valeriani, M., de Tommaso, M., Restuccia, D., Le Pera, D., Guido, M., Iannetti, G.D., Libro, G., Truini, A., Di Trapani, G., Puca, F., Tonali, P., Cruccu, G., 2003. Reduced habituation to experimental pain in migraine patients: a CO(2) laser evoked potential study. *Pain* 105, 57–64. [https://doi.org/10.1016/s0304-3959\(03\)00137-4](https://doi.org/10.1016/s0304-3959(03)00137-4).
- Wager, T.D., Davidson, M.L., Hughes, B.L., Lindquist, M.A., Ochsner, K.N., 2008. Prefrontal-subcortical pathways mediating successful emotion regulation. *Neuron* 59, 1037–1050. <https://doi.org/10.1016/j.neuron.2008.09.006>.
- Wang, W., Timsit-Berthier, M., Schoenen, J., 1996. Intensity dependence of auditory evoked potentials is pronounced in migraine: an indication of cortical potentiation and low serotonergic neurotransmission? *Neurology* 46:1404–1409. doi:10.1212/wnl.46.5.1404.
- Wei, H.-L., Chen, J., Chen, Y.-C., Yu, Y.-S., Zhou, G.-P., Qu, L.-J., Yin, X., Li, J., Zhang, H., 2019. Impaired functional connectivity of limbic system in migraine without aura. *Brain Imaging Behav.* <https://doi.org/10.1007/s11682-019-00116-5>.
- Wilcox, S.L., Veggeberg, R., Lemme, J., Hodkinson, D.J., Scrivani, S., Burstein, R., Becerra, L., Borsook, D., 2016. Increased functional activation of limbic brain regions during negative emotional processing in migraine. *Front. Hum. Neurosci.* 10, 366. <https://doi.org/10.3389/fnhum.2016.00366>.
- Wilkinson, G.N., Rogers, C.E., 1973. Symbolic description of factorial models for analysis of variance. *Appl. Stat.* 22, 392. <https://doi.org/10.2307/2346786>.